

Fast chemical sensor for eddy-correlation measurements of methane emissions from rice paddy fields

Peter Werle and Robert Kormann

A high-frequency-modulation spectrometer with a lead-salt diode laser operating in the ν_4 band of CH_4 at $7.8 \mu\text{m}$ was used as a fast chemical sensor to measure ambient methane concentrations of 2 ppmv (parts in 10^6 volume-mixing ratio) with a time resolution of 10 Hz for micrometeorological flux measurements. To assess the quality of the data on methane emissions from rice paddy fields, we compared eddy-correlation measurements with simultaneously recorded emission data from the state-of-the-art closed-chamber technique and showed that the closed-chamber measurements were 60%–90% higher than were the eddy-correlation measurements during the campaign. This outcome demonstrates that diode-laser spectroscopy is a valuable tool for quality assurance. © 2001 Optical Society of America

OCIS codes: 010.1120, 010.1330, 010.3920, 120.0120, 140.2020, 300.6270.

1. Introduction

Methane is emitted into the atmosphere from natural sources including wetlands, oceans, termites, and CH_4 -hydrate destabilization in permafrost regions.^{1,2} Analyses of air bubbles in ice cores suggest that the atmospheric concentrations of CH_4 remained fairly constant to as high as 700 ppbv (1 ppbv = 10^{-9} volume-mixing ratio) between 30,000 and 300 years ago.³ The atmospheric concentration of CH_4 has more than doubled since the industrial revolution⁴ to approximately 1.7 ppmv (1 ppmv = 10^{-6} volume-mixing ratio). The increase in the atmospheric CH_4 concentration during the past century is positively correlated with the growth of the world's human population, and it appears that anthropogenic activities, including agriculture intensification, biomass burning, and natural-gas drilling, have a strong influence on CH_4 emissions.⁵ In addition to increased emissions of CH_4 there appears to be a less efficient removal of CH_4 from the atmosphere.⁶

Among biogenic sources of atmospheric CH_4 , rice

paddies have been identified as one of the most important sources. Methane is produced in rice paddy fields by the strictly anaerobic process of methanogenesis catalyzed by methanogenic bacteria. Methane emissions from rice paddy fields contribute approximately 12%–20% to the overall atmospheric methane budget. Rice cultivars can strongly influence methane emissions from rice paddy fields, and therefore the use of rice cultivars that show low methane-emission rates in the field has to be regarded at present as one of the most promising realistic approaches to mitigating CH_4 emissions at sustainable rice production.

In the future CH_4 is expected to become an increasingly important greenhouse gas, as Asian rice production must increase by 60% over the next 30 years to keep up with population growth.⁷ Increased rice-cropping intensity and fertilizer use are expected to increase significantly CH_4 emissions from flooded rice paddies.⁸ The projected concentration^{9,10} of CH_4 by the year 2030 is 2200 to 2500 ppbv.

To specify and implement effective CH_4 -reduction policies requires that more precise quantification of fluxes from individual sources be determined. In particular, there is a need to understand and assess CH_4 fluxes from rice paddies better because global extrapolations^{1,2} range from 25–150 Tg yr^{-1} . The global CH_4 -flux estimates from rice paddies have been extrapolated almost exclusively from closed-chamber measurements.^{11–15} In this process, small areas of a rice paddy field are enclosed within a gas-

P. Werle (PWWerle@aol.com) is with the Fraunhofer Institut (IFU), Kreuzeckbahnstrasse 19, 82467 Garmisch-Partenkirchen, Germany. R. Kormann is with the Max-Planck Institut für Chemie, Saarstrasse 23, 55020 Mainz, Germany.

Received 17 May 2000; revised manuscript received 24 August 2000.

0003-6935/01/060846-13\$15.00/0

© 2001 Optical Society of America

tight chamber, and the flux-rate calculation is based on the time-dependent linear increase of CH₄ in the closed chamber's atmosphere.¹⁶

An interdisciplinary research project funded by the European Community provided simultaneous measurements of methane emissions from rice paddy fields by the eddy-correlation and the closed-chamber techniques during field campaigns that were performed to assess and improve the quality of data on methane fluxes and allow a comparison with the data from continuous monitoring provided by the chamber method.

2. Fast Chemical Sensor for Methane-Flux Measurements

The report of the External Advisory Committee on an interregional research program on methane emission from rice fields¹⁷ recommended the inclusion of additional measurement techniques for methane emissions from rice fields along with the standard diffusion-chamber method. Of special interest is the use of micrometeorological techniques, especially those involving laser measurements, for measuring methane emissions.

A major limitation on atmospheric research on surface-exchange and flux measurements is the lack of sensitive, reliable, and fast-response chemical-species sensors.¹⁸ Therefore in past years techniques for fast and simultaneously sensitive trace-gas measurements based on tunable-diode-laser (TDL) absorption spectroscopy have been successfully applied to micrometeorological flux-measurement techniques, i.e., the eddy-covariance technique.^{19–25} The availability of such sensors offers a new approach to validating closed-chamber measurements and provides information about CH₄ emissions on a larger scale, which is the basis for any up-scaling effort.

The eddy-correlation technique directly determines the flux of an atmospheric trace constituent through a plane that is parallel to the surface. For the determination of surface-emission and surface-deposition fluxes the method is rigorous when specific criteria are met. Ideally, the meteorological conditions controlling the state of the turbulence should not vary over the course of the measurements. The surface viewed by the sensors should be horizontally uniform in both its physical and its chemical-biological aspects and should stretch for a distance much greater than the height z at which the measurements are made (the fetch is typically $100z$). This height z should be much greater than the scale of the surface roughness and the intrinsic scale of the sensors.

Because the eddy-correlation method can be considered to define the instantaneous upward or downward transport of the constituent and then to average the contributions to yield the net flux, it must take into account the frequency range of the turbulence for vertically transporting the constituents in the atmosphere. The technique requires simultaneous, fast, and accurate measurements of the vertical velocity and the trace species in question. Fortunately, a

technique for the measurement of the turbulence with the necessary resolution is available. Sonic anemometers can readily yield air-motion data with the required resolution. Likewise, the ability to handle the air-motion and the chemical-concentration data with modern computer systems is well in hand. Thus these aspects can be ignored, and the major limitation on field measurements can be dealt with: an appropriate chemical sensor with sufficient time and chemical resolutions.

Therefore a fast laser optical sensor is the key issue for eddy-correlation measurements. Diode-laser spectrometers are now at the threshold of routine application in environmental monitoring. To date, the development of this technology has been driven mainly by scientific questions, but increasingly these techniques are applied to a sensitive, selective, and fast analysis for monitoring applications.^{19–27}

The key element of the fast chemical sensor is the laser diode. In Fig. 1(a) the absorption spectrum of methane is plotted together with the atmospheric water absorption versus the wavelength. The near-IR absorption comprises overtone or combination bands that typically are 1 to several orders of magnitude weaker than the IR fundamental band. Antimonide lasers²⁶ can be used for the detection of CH₄ at 3.26 μm (ν_3), and for the 7.8- μm (ν_4) spectral region lead-salt diode lasers are the optimum choice, as they cover the IR fundamental bands with strong absorption for the most atmospheric trace gases.

In trace-gas monitoring applications lead-salt laser instruments routinely achieve parts-per-billion detection levels of a number of important molecular species.²⁷ When one starts to select a laser the first task is to select from mode maps, as shown in Fig. 1, a combination of a base temperature and a drive current at which the laser produces a strong, preferably single-mode, emission that is tuned to the absorption line being monitored. After the investigation of several antimonide and lead-salt diode lasers a lead-salt device with the characteristics shown in Fig. 1 was selected. For injection currents between 400 and 600 mA at temperatures ranging from 85 to 95 K, single-mode operation with an average power level of 200 μW was ensured, and isolated methane-absorption lines could be selected reproducibly for the measurements even after repetitive thermal cycling, which was an important criterion for the planned field measurements.

As a high time resolution and a high chemical resolution were prerequisites for the success of the measurements, high-frequency-modulation (high-FM) spectroscopy was selected. In FM spectroscopy the laser is modulated at higher frequencies, typically in the rf region, thus allowing selective and fast scanning over an absorption line of a molecule. The technique is described in detail in a recent review.²⁷

The layout of the detection electronics is shown in Fig. 2(a). The system can be run in either the single-tone or the two-tone mode, and the optimum method can be selected by the system operator from case to case, depending on the experimental conditions.

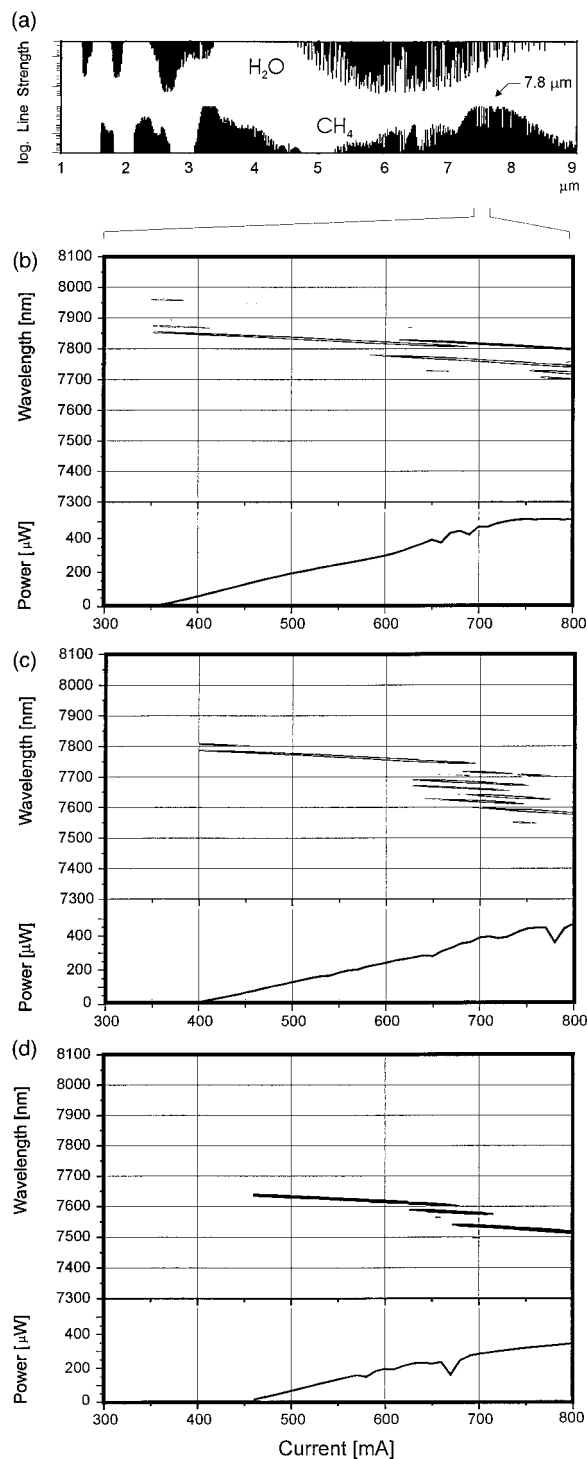


Fig. 1. (a) Absorption spectrum of CH₄ and atmospheric water plotted versus the wavelength. For sensitive detection of methane the spectral ranges at approximately 3.3 μm (for ν_3) and 7.8 μm (for ν_4) are well suited. A lead-salt device operating near 7.8 μm was selected. For injection currents between 400 and 600 mA at temperatures of (b) 85 K, (c) 90 K, and (d) 95 K, single-mode operation with an average power level of 200 μW was ensured.

The modulation section provides the required rf modulation for the laser. The laser beam is split into a sample and a reference path. Detector signals are fed into phase-sensitive detection electronics, which

can be regarded as a high-frequency lock-in amplifier. Both signals (sample and reference) are then digitized and further processed by use of digital filters and line-locking, normalization, and calibration procedures.²⁸

The reference beam passes through a reference cell, which provides a high signal-to-noise ratio signal from the spectral feature under investigation. This channel is used for line-locking and on-line drift correction. A line-locking procedure monitors the deviation of the signal position from a given set point and decides whether a change in temperature or current has to be made to compensate for drifts. To compensate for fast and small fluctuations requires that the signals be on-line shifted prior to signal averaging, as shown in Fig. 2(b). These corrected signals are then fed into a digital filter routine that removes the background and references the signal to a previously stored calibration signal, as shown in Fig. 2(c). All algorithms and procedures were implemented in a real-time parallel multiprocessor system. With this spectrometer ambient methane concentrations of approximately 2 ppm can be detected with a precision of approximately 1% at a 10-Hz repetition rate.

The optical layout together with the external control units of the system based on the detection scheme described above are shown in Fig. 3. The optomechanical components of the spectrometer are mounted on a 50 cm × 90 cm optical breadboard. The lead-salt diode laser is mounted on a cold head within an LN₂ Dewar laser (Laser Photonics, Inc., Analytics Division, Andover, Massachusetts, Model L5736 Laser Dewar). The diverging laser beam is collimated to a nearly parallel beam (labeled with a circled numeral 1 in Fig. 3) by an off-axis parabola, which focuses the beam at the center of a commercial astigmatic Herriott cell (New Focus, Inc., Santa Clara, California, Model 5611 multipass cell) with a total path length of 18 m. This cell has a very small internal volume of 0.3 l and is specially designed for applications requiring a high time resolution. The outgoing thin and nearly parallel beam (labeled with a circled 3) is then focused onto a broadband HgCdTe measurement detector by use of a BaF₂ planoconvex lens. The reflex of the cell-inlet window is used as a reference (labeled with a circled 2) after passing through a small cell that contains pure methane gas. This reference beam is used, on the one hand, for the reliable identification of the absorption features of the trace gas of interest and, on the other hand, for the active stabilization (line locking) of the spectrometer.

A visible (680-nm) diode laser is used to align the system. The beam splitter, which sets the alignment beam onto the main light path, is removed during the measurement. A rotary vacuum pump (Leybold AG, Köln, Germany, Model SOGEVAC SV 65) provides a gas flow of approximately 18 standard liters per minute (slpm) through the Herriott cell at a pressure of approximately 50 hPa. A dust filter is mounted at the inlet point of the measurement head to protect the gas system, and especially the mirrors

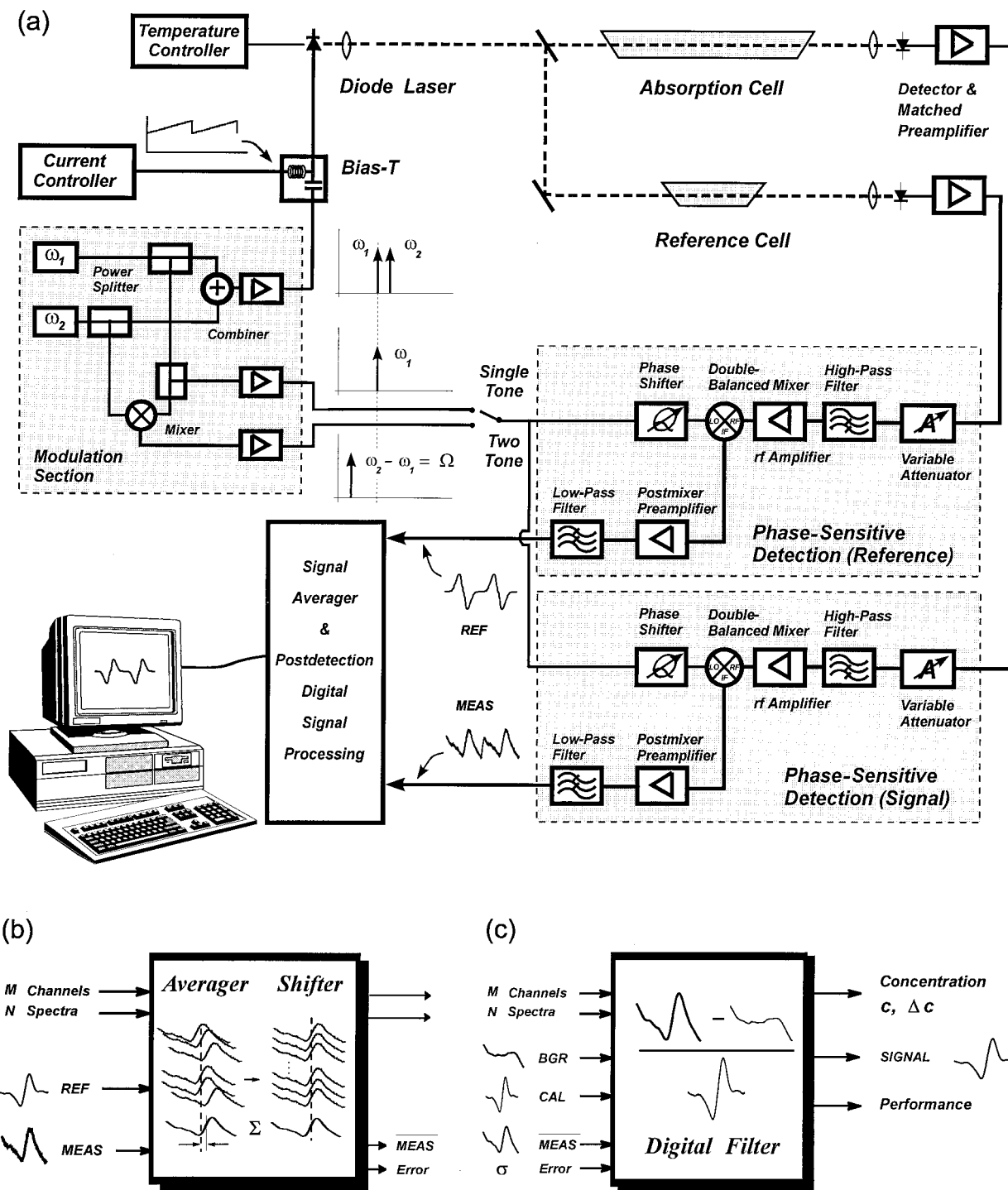


Fig. 2. (a) Signal-processing scheme with the implementation of the single-tone and the two-tone techniques. The main elements in the data processing are signal averaging, filtering, intensity normalization, and line locking. (b) Prior to signal averaging all spectra were drift corrected. (c) The digital filter processes background corrections. REF, reference signal; MEAS, measured signal; \overline{MEAS} , averaged measured signal; BGR, background signal; CAL, calibration signal.

of the Herriott cell, from pollution. A newly developed calibration system allowed programmed sequences of measurements of the background signals (N_2), the calibration gas, and the ambient air. The calibration system is based on a dilution system, and high-concentration calibration gas from steel cylinders is diluted to ambient concentrations.

Fast examination of the wind vectors was performed by use of an ultrasonic anemometer (Gill Instruments, Ltd., Lymington, Hampshire, UK, Model 1012R2 Solent Research ultrasonic anemometer). It was operated in the calibrated mode, meaning that the results were corrected for damping of the wind velocity that was caused by the anemometer mount

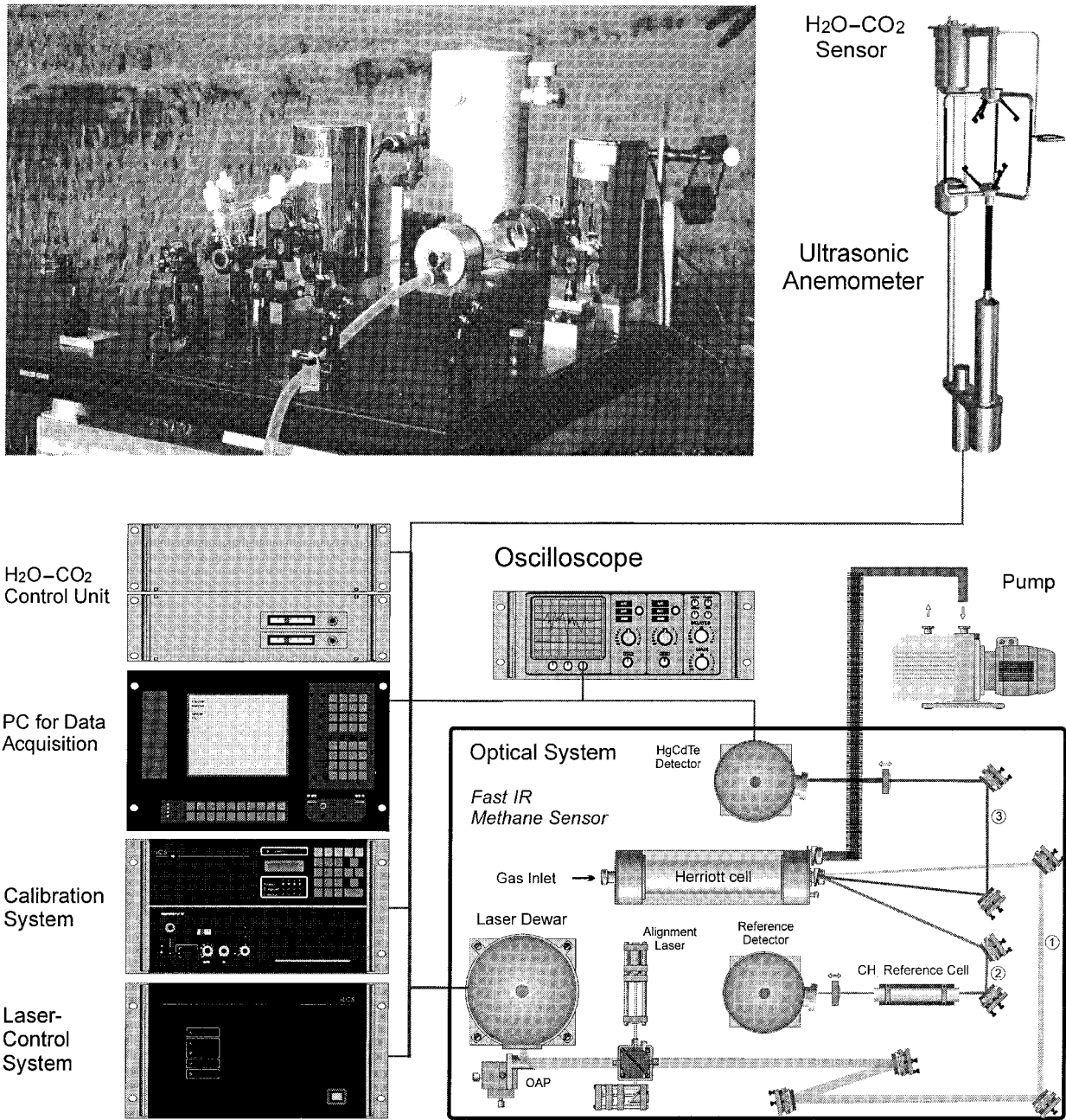


Fig. 3. High-FM spectrometer for methane sensing with all the control electronics for eddy-correlation trace-gas flux measurements together with the layout of the optical sensor that is based on a small-volume (0.3-l) Herriott cell. The nondispersive IR H_2O-CO_2 sensor is mounted behind the measurement paths of the ultrasonic anemometer and the gas inlet for the spectrometer. OAP, off-axis parabola.

by use of a built-in calibration procedure. The speed of sound, also determined by the anemometer, was used to derive the virtual temperature. Fast water-vapor and carbon dioxide measurements were performed by use of an open-path nondispersive IR device (Advanet, Inc., Okayama, Japan, Model E009 infrared gas analyzer), which is shown together with the anemometer in the upper right-hand section of Fig. 3.

A prototype of the commercial H_2O-CO_2 device is described by Othaki and Matsui.²⁸ The band limit of the measurement device was found to be approxi-

mately 10 Hz on the basis of the approximations of Moore.²⁹ To avoid aliasing, we low-pass-filtered the signal of this device by using a four-pole Butterworth filter (a band limit of 10 Hz) before it was digitized by the spectrometer's data-acquisition system. To avoid band limiting by larger distances between the different measurement devices, we mounted them as close as possible to each other, keeping in mind that mutual perturbation can be possible.

The impact of the H_2O-CO_2 sensor and the gas inlet on the wind measurement by the shadowing of the wind seems to be low because, at the height of the

wind-measurement volume, only smaller construction elements are present. A shadowing effect by the additional devices (H_2O-CO_2 sensor, spectrometer's gas inlet, etc.) is also minimized by use of down-wind mounting from the expected main wind direction. Because the gas flow into the inlet of the spectrometer can also cause a nonvanishing wind velocity, the distance from the gas inlet to the wind-measurement zone (17 cm) was chosen such that the estimated influence was less than the resolution of the anemometer. To avoid an unwanted inclination of the anemometer, we equipped the measurement head with an inclinometer (Applied Geomechanics, Santa Cruz, California, Model 900-T biaxial clinometer) that allows a vertical adjustment of the measurement head within the geopotential. Neither drifts nor fluctuations nor relevant inclinations of the measurement head during the field measurements could be detected.

The measurement height was 3.2 m, which should allow a thorough observation of the inertial subrange for a typical wind velocity of 1.6 m/s. The measurement interval of the ultrasonic anemometer was fixed at 48 ms, corresponding to a measurement rate of approximately 20.8 Hz. The spectrometer integration time was set to 96 ms, which could then easily be synchronized with the data rate of the anemometer and which was adapted to the possible frequency resolution that is given by the gas exchange in the measurement cell of the spectrometer. The averaging time scale for the turbulent fluxes²¹ was chosen to be approximately 30 min, interrupted by a calibration procedure of the diode-laser spectrometer that lasted for approximately 20 s.

The system described so far is capable of measuring simultaneous wind and ambient methane-concentration data at a 10-Hz sampling rate. Such fast-response measurements of state variables generate time-series data that can be analyzed statistically. The general data-analysis scheme is shown in Fig. 4. Problems with the time series must be corrected before performing the eddy-correlation calculations. The data should be detrended and high-pass filtered to remove wavelengths longer than approximately 1/3 to 1/5 of the length of the series. This procedure ensures that enough complete cycles of the retained wavelengths are averaged to yield satisfactory statistics. Finally, we are left with a clean series that can be used in eddy-correlation analysis.

The first step in the eddy-correlation process is then to calculate the perturbation values of the data points. For the measured time series of concentration values, we can subtract the mean from each data point to yield the time series of perturbations c' . We can similarly find a time series of the vertical wind-velocity perturbations w' . Multiplying the respective values together yields a time series $w'c'$. The average of this series, $\langle w'c' \rangle$, gives the turbulent vertical flux. An advantage of this method is that it is direct and simple, and fluxes can be calculated at whatever height or location the original time series

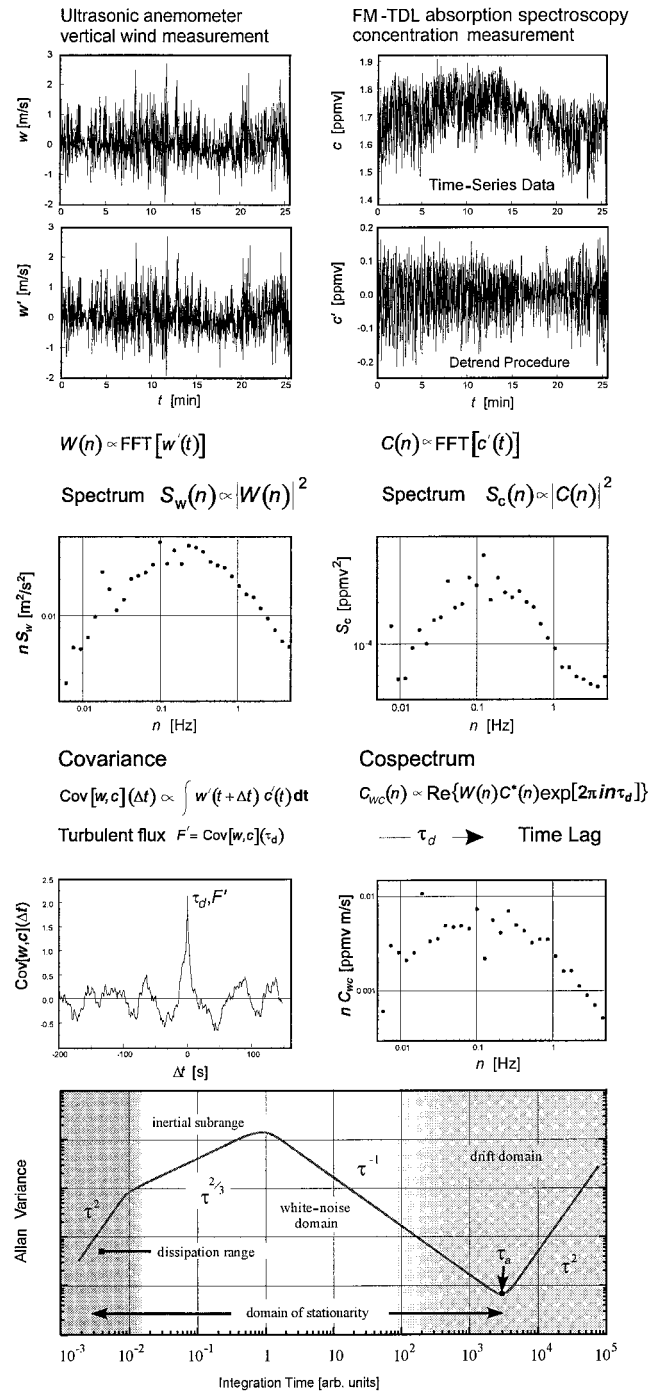


Fig. 4. Schematic illustration of the data analysis: Raw data from the sonic anemometer and the spectrometer were detrended, and the covariance and the cospectra were calculated to determine the time lag τ_d between the wind and the concentration measurements. An Allan variance analysis³⁸ was used to check the stationary conditions.

was measured. The trace-gas devices used within the described measurement campaign measure densities or mass per volume (H_2O-CO_2 sensor) as well as (mass) mixing ratios (TDL methane sensor) with respect to moist air. According to Webb *et al.*,³¹ a correction, which was found to be of the order of 10%,

has to be applied. Predrying of the air before quantifying the mass mixing ratio would have avoided this correction but might limit the frequency resolution of the concentration-measurement system.

Data conditioning also covers a rotation of the wind vectors and a trend removal. Consecutive rotations could be performed on each measured wind vector, those rotations constituting a linear rotation in accord with the instantaneous inclinometer reading, a rotation around the z axis (which causes the horizontal component of the average wind velocity to point along the positive x axis, and rotations that cause the mean vertical wind to vanish.³² By adoption of a systematic error of 3% per degree,³³ these errors should be kept well below 10%.

Because of technical limitations, a sporadic loss of individual measurement points could appear. For these cases linear interpolation from neighboring points was implemented in the analysis software. The flow of the ambient air into the measurement cell of the spectrometer introduces an uncertainty into the simultaneity of the time-series data. Therefore a correlation analysis was used to find the time lag and the fluxes.^{34,35} The standard deviations within the covariance plots for longer time lags were used to estimate the measurement error. This method takes into account both the real measurement errors of the individual data points and the uncertainty in the stationarity during the averaging time interval, and it turned out to be a very conservative measure for the errors of the turbulent fluxes.

The Fourier-transformed time series were used to derive spectra.³⁶ Cross spectra, cospectra, and quadrature spectra, as well as coherence spectra, were found by use of the time delay derived from the correlation analysis. These spectra were averaged by use of exponentially grown frequency intervals to account for the usually logarithmic representation of the spectra. They showed that the considered frequency range between approximately 0.003 and 5 Hz contained the main contributions to the turbulent fluctuations and fluxes.

Trends of the micrometeorological time series, caused mainly by system drifts and by micrometeorological instationarities themselves, must be removed before starting the flux calculation. This procedure is usually performed by use of a running mean or a band limit, as was done in this study. The high-pass time constant was determined based on the Allan variance criterion.³⁷ An Allan plot,³⁸ shown in the lower section of Fig. 4, provides complementary time-domain information to the frequency domain.³⁶ The minimum in the Allan variance at τ_a corresponds to the optimum integration time, which is a characteristic property for a given data set because it represents the time during which we can assume stationary conditions for the data set under investigation.³⁸ Stationarity of the micrometeorological time series was typically guaranteed for several hundred seconds. Accordingly, the detrend time constant was chosen to be fixed at 300 s.

3. Field Measurements

Methane emissions from rice paddy fields in Italy have been investigated for several years and show strong diurnal and seasonal variations with significant differences in consecutive years.^{13,14} Usually, such measurements are based on gas-collector chambers. A typical gas-collector chamber is made of colorless, smooth plexiglass. The edges are fixed by aluminum profiles and are sealed with silicone on the inside. A chamber covers a surface area of approximately 0.4 m² and is approximately 90 cm high. Each chamber is fitted with a removable plexiglass cover, the position of which is controlled by a pneumatic pressure cylinder. A fan mounted on the inside of the cover causes rapid replacement of the air inside the chamber with ambient air when the cover is open. When the cover is closed a fan causes the rapid mixing of the air within the chamber so that vertical gas gradients inside the chamber are avoided.

The gas-collector chamber is placed in the field on stainless-steel frames that are sunk into the soil prior to flooding and remain in the same position during the entire vegetation period. The inner volume of the chamber is separated from the ambient atmosphere, but the water in the chamber can undergo exchange with the surrounding water body.

The CH₄-emission rate is calculated from the temporal increase of the CH₄ concentration inside the box. The concentration increases during the typically 30-min closure time and is measured with a gas chromatograph that is connected to a computer through an interface designed for peak integration.¹⁶

An automated system for methane-flux measurements that is based on the closed-chamber method was developed by F. Conen from the Institute of Ecology and Resource Management (University of Edinburgh). It allowed continuous measurements at eight different locations for an entire growing season, as is necessary for obtaining data on diurnal and seasonal variations in emission rates under field conditions.

The field work was carried out at the Istituto Sperimentale per la Cerealicoltura, Sezione Specializzata per la Ricoltura, Vercelli, Italy. The institute is located in the main rice-growing area of Western Europe: This area covers a more than 2000-km² rice-growing area in northern Italy in the valley of the River Po between the cities of Milan and Turin. The site is rather homogenous and is covered with rice paddy fields of different plot sizes, so a good fetch for eddy-correlation measurements was provided.

In times of high CH₄-emission rates from rice paddy fields (from May to August) intensive measuring campaigns were performed by use of both the closed-chamber method and the eddy-correlation technique. For the field eddy-correlation measurements a trailer containing the fast laser optical sensor for methane-flux measurements was prepared for operation at the measurement site in Vercelli [Figs.

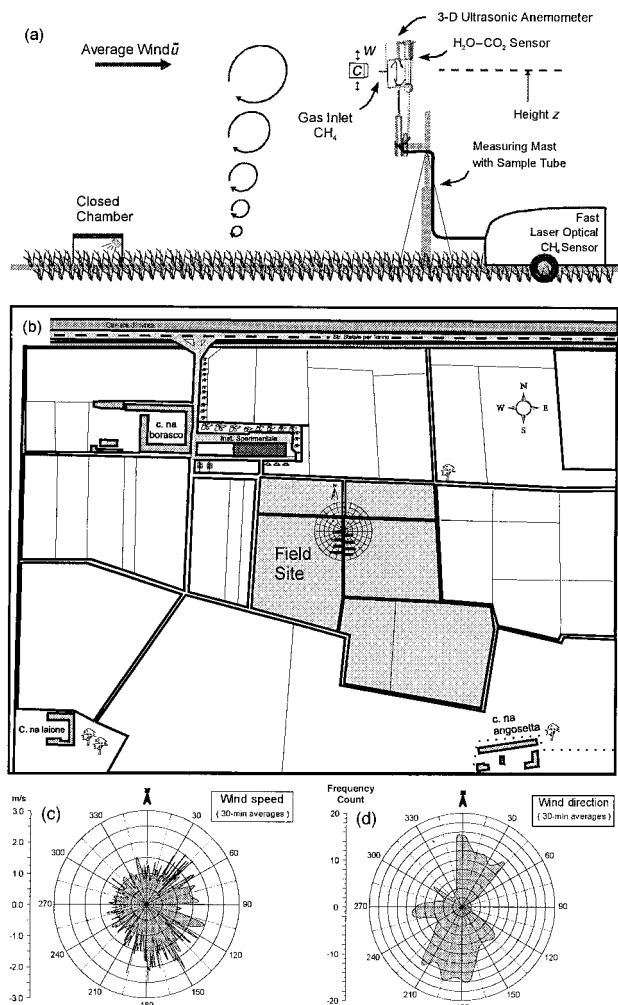


Fig. 5. (a) Setup for the field eddy-correlation and the closed-chamber measurements. 3-D, three dimensional. (b) Measurement mast located in the downwind direction that was north of the closed chambers in the center of the field with several hundred meters of fetch in all southern directions. The distributions of (c) the wind speed and (d) the wind direction at the site. Shown is a pronounced north-south distribution of the wind directions with winds from the Mediterranean sea moving toward the Swiss alps.

5(a) and 5(b)]. The instrument was remote controlled through an ethernet connection to the institute. A variable-height measurement mast for the measurement of the meteorological data and continuous gas sampling was set up in the field. The whole system was backed up by an uninterrupted power supply, and residual-current detectors were implemented for safety reasons.

Wind direction, wind speed, temperature, pressure, humidity, and other factors were recorded together with the spectroscopic gas-sensor data to generate a complete data set for micrometeorological analysis. In general, the best wind conditions for eddy-correlation measurements with wind speeds well above 1 m/s and predominantly coming from south of the measurement mast (where the chambers were located) were found from noon to early after-

noon. Data were recorded for daytime and for 24-h flux measurements.

In total more than 300 measurements of 30-min intervals each provided data for the flux determination on the basis of a 10-Hz temporal resolution. These measurements were digitized and stored for off-line analysis. The three wind components (two horizontal and one vertical) yielded horizontal wind speeds and directions [Figs. 6(a) and 6(b)], and the methane data provided a time stamp for off-line analysis. A total of 36,000 wind vectors at a 20-Hz rate plus 18,000 data points at a 10-Hz rate for methane, the measurement error, the temperature, and a series of parameters for data quality control were obtained for each 30-min interval. The total data coverage during the campaign was better than 95%. The separately recorded data [Fig. 6(d)] from the Solent Research ultrasonic anemometer and the diode-laser methane sensor [Fig. 6(e)] were combined into one data set for further processing of the methane flux $w'c'$ [Fig. 6(g)]. The time lag between the sonic-anemometer data and the gas analyzer that is due to the finite length of the sampling tube was determined for each of the 300 measurement intervals, and the data sets were corrected by a relative shift of the data to obtain coincident data for the final flux determination. The covariance of the flux plotted versus the time delay is shown in Fig. 6(f). The peak corresponds to the corrected time delay and therefore to the observed turbulent flux. The usual sign convention, meaning an upward-pointing z axis, was used. Therefore a maximum corresponds to an input of the quantity into the atmosphere. Some nonrandom fluctuations for large time delays can also be seen in this type of plot. Such low-frequency fluctuations typically were observed during unstable stratification. As was already mentioned, the estimated errors from the covariance plots contain, of course, these low-frequency fluctuations.

For each 30-min interval the corresponding spectra for the vertical wind and the concentration as well as the cospectra of the flux were calculated and analyzed to check whether the whole flux was obtained. This process is important to ensure that no significant flux contributions in the high-frequency (sensor bandwidth limited) and in the low-frequency (measurement time limited) domains are lost and that fluxes will not be underestimated.³⁶ The inertial subrange with its expected $n^{-4/3}$ behavior can clearly be seen within the cospectrum $nC_{w'c'}$ of the fluctuations of the vertical wind and the methane concentration [Fig. 6(h)].

An Allan variance analysis [Fig. 6(i)] was performed to ensure the stability of the data set prior to data averaging.^{37,38} It is interesting to note the behavior of the Allan variance in the presence of turbulence at short integration times for which there is practically no real averaging. Therefore we assume a data set in which a turbulence parameter has been recorded. If the sampling frequency is sufficiently high that fast fluctuations can be well resolved the Allan variance at first detects a kind of linear drift

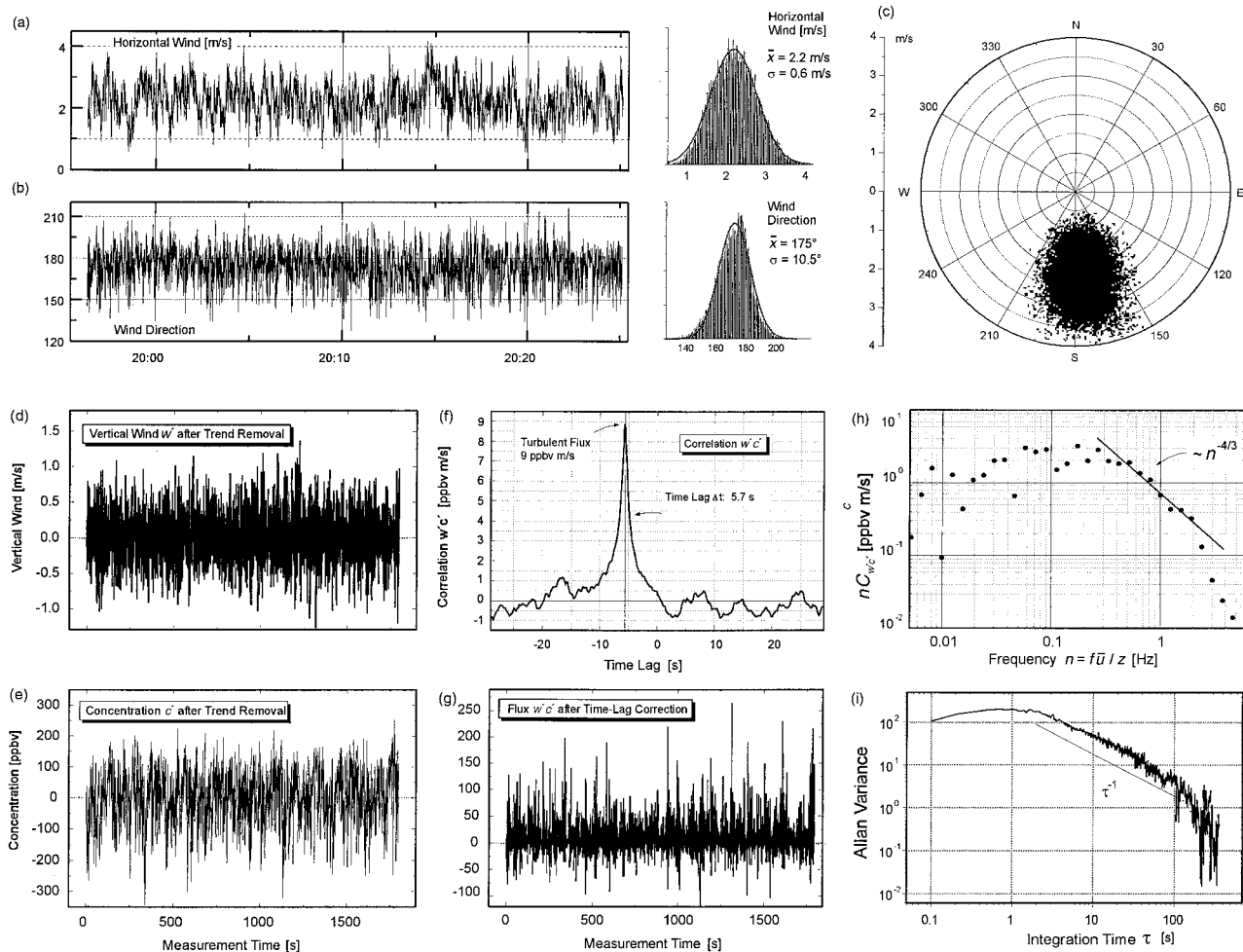


Fig. 6. Time-series data for (a) the horizontal wind direction and (b) the wind direction. (c) A polar plot of both wind directions that illustrates stable conditions. The measurement mast was located in the center of the polar plot. Detrended time-series data of the fluctuations of (d) the vertical wind w' and (e) the CH_4 concentrations c' as determined at a 10-Hz rate. (f) After a time-lag correction, (g) the corresponding flux $w'c'$ was calculated. (h) Spectra that were analyzed to guarantee that the high-frequency part of the flux was completely measured,³⁶ and (i) an Allan variance analysis after the application of a detrending procedure confirmed the stability for averaging.^{37,38}

and starts with a slope of 2. This slope changes in the inertial subrange in which frequency fluctuations according to $f^{-5/3}$ dominate the Allan plot, and the slope becomes approximately $2/3$. As primarily $1/f$ noise dominates for longer integration times, we end up with a constant level for the Allan variance. If the integration time is sufficiently long to permit integration over the fast fluctuations they will contribute less and less to the longer integration times and the white noise, as the dominant noise source will now be averaged, leading to a decreasing Allan variance (Fig. 4) to a point at which the drift effects start to influence the measurement, i.e., the stationarity of the measurement is no longer valid.

The data were edited to match several quality-assurance criteria, e.g., minimum wind speed, stable meteorological conditions, and wind coming from the southern directions where the chambers are located. One week of such final flux data is shown in Fig. 7(a); each individual data point is based on a set of data, as

shown in Fig. 6. During one week, the increasing flux was strongly correlated with the ambient temperature, and even a weak daily cycle with flux peaks in the early afternoon was observed. The calculated mean daytime flux for this period was 6.35 ppbv m/s, corresponding to 14.5 mg/(m² h). Figure 7(b) shows these fluxes plotted versus the wind direction during the measurement interval that was determined from the time-series data sets, as shown in Fig. 6. We also estimated the footprint of the eddy-correlation measurements, as discussed by Schuepp,³⁹ and obtained the peak of the emissions, as indicated by the filled circles in Fig. 7(c) in which the footprint is plotted versus the wind direction. The peak emissions cover the area where the eight automatic chambers were located well. The radial lines in the plot indicate the area from which approximately 50% of the flux is expected to come. Even if this approximation typically overestimates the footprint the

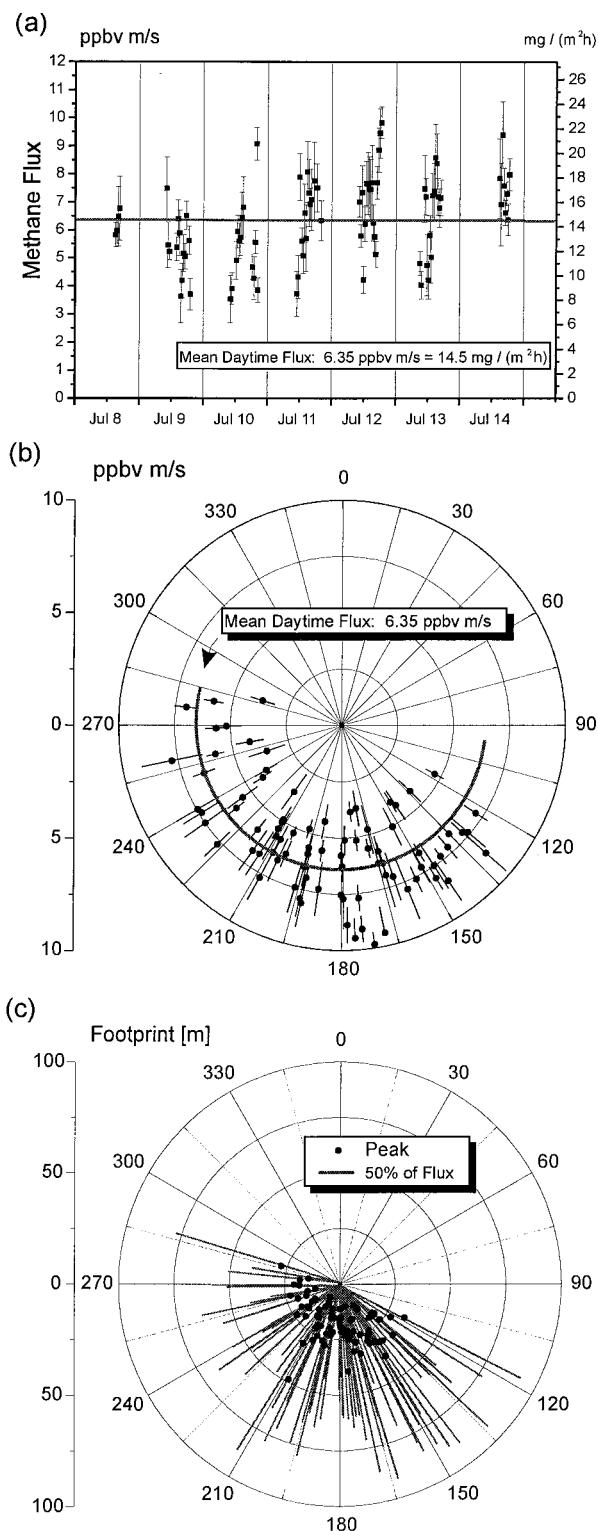


Fig. 7. (a) Time-series data of the methane flux plotted versus (b) the wind direction and (c) the corresponding footprint as indicators for the overlap of closed-chamber data and eddy-correlation measurements.

eddy-correlation measurements are representative for the field area under investigation.

A set of high-quality data on methane emissions from irrigated rice paddy fields in Italy was collected

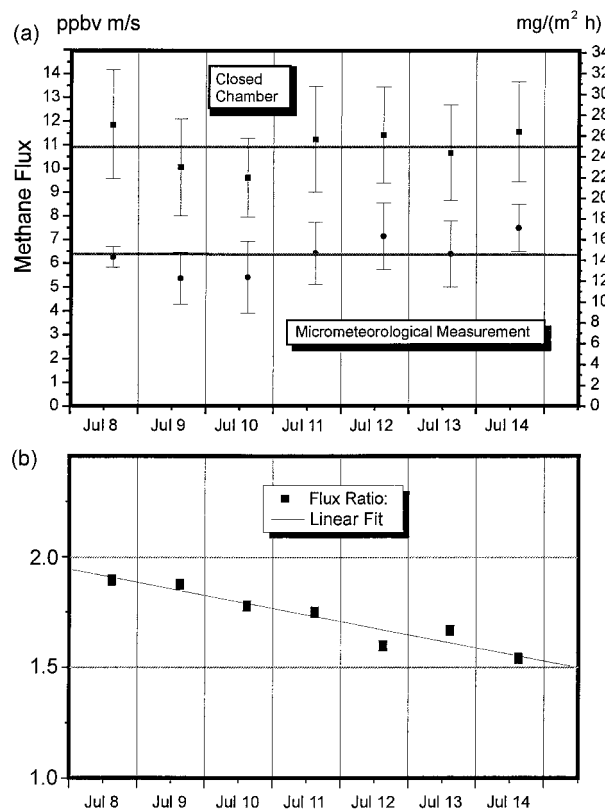


Fig. 8. (a) Methane fluxes derived from measurements obtained by use of the closed-chamber (filled squares) and the eddy-correlation, i.e., micrometeorologic, (filled circles) methods. The straight lines at 11 and 6.5 on the left-hand axis are for orientation only. (b) Decrease in the ratio of the closed-chamber measurements to the eddy correlation with time. This decrease indicates that 60%–90% higher fluxes were obtained with the closed-chamber measurements during the measurement period.

during the field campaign. From these data a mean daytime flux of 6.35 ppbv m/s [14.5 mg/(m² h)] was derived. Figure 8(a) shows the daytime averages that were calculated from the data shown in Fig. 7(a) together with the averaged data from the corresponding closed-chamber measurements. The ratio of the fluxes that were calculated from the closed-chamber measurements and from the eddy-correlation measurements is plotted in Fig. 8(b), and approximately 60%–80% higher methane emissions were determined by the closed-chamber method. The generally lower emission measurements of the laser-based micrometeorological eddy-correlation system shown here were confirmed in an on-site comparison with two other independent diode-laser-based instruments: A two-tone FM instrument³⁴ developed at the Max-Planck Institut, Mainz, Germany, was operated together with the instrument described here. In addition, a commercial fast-scanning IR spectrometer⁴⁰ (Aerodyne Research, Inc., Billerica, Massachusetts) of the Joint Research Center of the European Community, Ispra, Italy, also provided eddy-correlation data from the same site during the campaign. All systems have independent calibration

systems and optical designs, different sampling tubes and inlet systems at different measurement heights, specific control hardware and software, and individually written eddy-correlation data-analysis procedures.

4. Summary and Discussion

TDL absorption spectroscopy based on the FM technique is one of the most powerful spectroscopic techniques for the ultrasensitive and high-speed detection of weak absorption signals. TDL absorption spectroscopy has made the transition from a technique that was mainly of interest to instrument developers into one that produces results of real value to trace-gas analysis and atmospheric-chemistry studies. This technique is especially well suited to the measurement of trace-gas fluxes from terrestrial ecosystems on the basis of the eddy-correlation technique because it allows rapid measurements of ambient gas concentrations of approximately 2 ppmv with frequencies as high as 10 Hz with an accuracy that is still better than 1%.

In the context of an interdisciplinary research project eddy-correlation measurements of methane emissions from rice paddy fields have been performed during a field campaign to permit a comparison with data from continuous monitoring provided by the closed-chamber technique. The application of these two independent methods should help to assess and improve the quality of the data on methane fluxes. The closed-chamber technique yields valuable results for understanding the local processes that finally lead to net methane emissions into the atmosphere and the detection of diurnal as well as seasonal variations in CH₄-flux rates from rice paddy fields. It is appropriate to determine the effects of different site treatments on fluxes, but site spatial variability is a great problem when using chambers to measure fluxes from a field or an ecosystem.⁴¹ In addition, chambers disturb the natural air turbulence, decouple the rice plant from the ambient turbulent atmosphere, and alter the temperature, the solar radiation, and the gas concentrations in the measurement environment. Therefore the extrapolation of CH₄ emissions on the basis of flux rates that are obtained by use of small closed-chamber measurements to field, landscape, and regional levels is not established very well. A major objective of the eddy-correlation measurements was the exploration of systematic differences between the state-of-the-art closed-chamber method and a direct micrometeorological technique.

During the measurement campaign a record of high-quality data on methane emissions from irrigated rice paddy fields in Italy has been obtained. From the eddy-correlation measurements a mean daytime flux of 6.35 ppbv m/s [14.5 mg/(m² h)] has been derived, whereas the measurements based on the state-of-the-art closed-chamber technique have reported approximately 60%–90% higher methane emissions. The lower fluxes measured by the laser-based micrometeorological eddy-correlation system shown here have been confirmed in on-site compari-

sons with two other independent diode-laser-based eddy-correlation systems. All participating instruments (laser spectrometers and gas chromatographs) were calibrated routinely, and simultaneous measurements of ambient methane *concentrations* have reported the same values. It is important to point out that the differences occurred for only the *fluxes* that were calculated from the different techniques.

As a first attempt to try to explain this difference, we should recall that closed chambers usually have a fan mounted inside the chamber, and when the chamber is closed the fan causes rapid mixing of the air within the chamber. Thus a strong artificial turbulence is introduced into the chamber that does not allow natural gradients to form inside the box. The chamber data may suffer from this experimentally introduced effect, which might have influenced the methane-flux measurements obtained with closed chambers in rice paddy fields to date.

During the analysis of the campaign data a positive correlation between the measured methane flux, the friction velocity, the horizontal wind, and the temperature has been found. This result is also in line with the recent findings of Kahlil *et al.*,⁴² who analyzed a 7-year data set on methane emissions from rice fields in Tu Zu, China, and found that greater wind speeds tend to result in greater methane emissions. They conclude that wind can affect fluxes from rice fields by an increase in the agitation of the soil and the water as the plants are moved in the wind, and this effect may be larger in windier locations. Although the amount of distortion or turbulence is constant inside the chamber and is decoupled from the atmospheric conditions, this is not the case for the almost unaffected *in situ* eddy-correlation measurements in the free atmosphere. As we can see from other available data, the decreasing ratio of the flux measured by the closed-chamber technique to the flux measured by the eddy-correlation technique during the week, as shown in Fig. 8(b), correlates well with the simultaneously increasing horizontal wind speed and friction velocity, which is a measure of turbulence. This finding indicates that, for higher wind speeds, the difference between the eddy-correlation data and the closed-chamber measurements becomes smaller, but, unfortunately, in the rice-growing region the wind speeds tend to be low and a problem remains: Do closed-chamber measurements overestimate methane emissions from rice paddy fields? Or do the independent eddy-correlation measurements underestimate the fluxes? Whatever the process is that causes more flux in the closed chamber with the fans on, to date the consensus of the project partners is that it accounts for only a fraction of the difference between chamber and micrometeorological measurements. The discrepancy between micrometeorological measurements and the closed-chamber technique has not yet been resolved completely. This issue is intended to be a major aspect of a future synthesis paper to aid in the interpretation of future CH₄-flux measurements by different methods.

This research was funded by the European community under contract PL970541-RICEOTOPES. For help, support, and stimulating discussions, we would like to thank our project partners K. A. Smith and F. Conen from the Institute for Ecology and Resource Management, Edinburgh, Scotland; D. Fowler from the Institute for Terrestrial Ecology, Edinburgh, Scotland; R. Mücke from the Fraunhofer Institute for Atmospheric Environmental Research, Garmisch-Partenkirchen, Germany; H. Fischer, F. Meixner, and T. Marik from the Department of Air Chemistry, Max-Planck Institute for Chemistry, Mainz, Germany; R. Conrad, P. Frenzel, and M. Krüger from the Max-Planck Institute for Terrestrial Microbiology, Marburg, Germany; G. Bidoglio, S. Cieslik, and A. Leip from the European Joint Research Centre Environmental Institute, Ispra, Italy; and, last but not least, Salvatore Russo from the Istituto Sperimentale per la Cerealicoltura, Vercelli, Italy. In particular, the continuing support on all micrometeorological aspects and the stimulating discussions with G. Kramm, Leipzig, Germany, and H. Müller, Hamburg, Germany, are gratefully acknowledged.

References and Note

- J. T. Houghton, G. J. Jenkins, and J. J. Ephraums, eds., *Climate Change: the Intergovernmental Panel on Climate Change (IPCC) Scientific Assessment* (Cambridge U. Press, New York, 1990).
- J. T. Houghton, B. A. Callander, and S. K. Varney, eds., *Climate Change 1992: The Supplemental Report to the IPCC Scientific Assessment* (Cambridge U. Press, New York, 1992).
- H. Craig and C. C. Chou, "Methane: the record in polar ice cores," *Geophys. Res. Lett.* **9**, 1221–1224 (1982).
- M. A. K. Kahlil and R. A. Rasmussen, "Atmospheric methane: recent global trends," *Environ. Sci. Technol.* **24**, 549–553 (1990).
- H. Schütz, W. Seiler, and R. Conrad, "Processes involved in formation and emission of CH₄ in rice paddies," *Biogeochemistry* **7**, 33–53 (1989).
- A. Mosier, D. Schimel, D. Valentine, K. Bronson, and W. Parton, "Methane and nitrous oxide fluxes in native, fertilized and cultivated grasslands," *Nature* **350**, 330–332 (1991).
- World Rice Statistics 1990* [International Rice Research Institute (IRRI), P.O. Box 933, Manila, Philippines, 1991].
- B. V. Braatz and K. B. Hogan, "Sustainable rice productivity and CH₄ reduction plan" (U.S. Environmental Protection Agency, Washington, D.C., 1991).
- T. E. Graedel and P. J. Crutzen, "The changing atmosphere," *Sci. Am.* **257**(9), 7–14 (1989).
- J. Lelieveld, P. J. Crutzen, and F. J. Dentener, "Changing concentration, lifetime, and climate forcing of atmospheric methane," *Tellus Part B* **50**, 128–132 (1998).
- R. J. Cicerone and J. D. Shetter, "Sources of atmospheric CH₄: measurements in rice paddies and a discussion," *J. Geophys. Res.* **86**, 7203–7209 (1981).
- W. Seiler, A. Holzappel-Pschorn, R. Conrad, and D. Scharffe, "CH₄ emission from rice paddies," *J. Atmos. Chem.* **1**, 241–268 (1984).
- A. Holzappel-Pschorn and W. Seiler, "CH₄ emission during a cultivation period from an Italian rice paddy," *J. Geophys. Res.* **91**, 11803–11814 (1986).
- H. Schütz, A. Holzappel-Pschorn, R. Conrad, H. Rennenberg, and W. Seiler, "A 3-year continuous record on the influence of daytime, season, and fertilizer treatment on CH₄ emission rates from an Italian rice paddy," *J. Geophys. Res.* **94**, 16405–16416 (1989).
- M. A. K. Kahlil, R. A. Rasmussen, M.-J. Wang, and L. Ren, "Methane emissions from rice fields in China," *Environ. Sci. Technol.* **25**, 979–981 (1991).
- D. Beever, O. van Cleemput, J. W. Czerkawski, M. Gibbs, K. Johnson, R. Leng, A. Mosier, W. H. Patric, Jr., J. Rowe, K. A. Smith, J. Wallace, and R. Wassmann, "Manual on measurement of methane and nitrous oxide emissions from agriculture," Rep. IAEA-TECDOC-674 (International Atomic Energy Agency, Vienna, Austria, 1992).
- H. P. Patrick, Jr., K. Minami, and R. L. Suss, "Report of the External Advisory Committee on an interregional research program on methane emission from rice fields" (International Rice Research Institute, Los Banos, Philippines, 1994).
- D. H. Lenschow and B. B. Hicks, eds., *Global Tropospheric Chemistry: Chemical Fluxes in the Global Atmosphere* (National Center for Atmospheric Research, Boulder, Co., 1989).
- I. J. Simpson, G. W. Thurtell, G. E. Kidd, M. Lin, T. H. Demetriades-Shah, I. D. Flitcroft, E. T. Kanemasu, D. Nie, K. F. Bronson, and H. U. Neue, "Tunable diode laser measurements of methane fluxes from an irrigated rice paddy field in the Philippines," *J. Geophys. Res.* **100**, 7283–7290 (1995).
- S. M. Fan, S. C. Wofsy, P. S. Bakwin, D. J. Jacob, S. M. Anderson, P. L. Keibian, J. B. McManus, C. E. Kolb, and D. R. Fitzjerald, "Micrometeorological measurements of CH₄ and CO₂ exchange between the atmosphere and subarctic tundra," *J. Geophys. Res.* **97**, 16627–16643 (1992).
- D. Fowler, K. J. Hargreaves, U. Skiba, R. Milne, M. S. Zahniser, J. B. Moncrieff, I. J. Beverland, and M. W. Gallagher, "Measurements of CH₄ and N₂O fluxes at the landscape scale using micrometeorological methods," *Philos. Trans. R. Soc. London* **351**, 363–370 (1995).
- R. Kormann, H. Müller, and P. Werle, "Eddy flux measurements of methane over the fen Murnauer Moos, 11°11'E, 47°39'N, using a fast tunable diode laser spectrometer," *Atmos. Environ.* (to be published).
- D. C. Hovde, T. P. Meyers, A. C. Stanton, and D. R. Matt, "Methane emissions from a landfill measured by eddy correlation using a fast response diode laser sensor," *J. Atmos. Chem.* **20**, 141–162 (1995).
- S. B. Verma, F. G. Ullman, D. Billesbach, R. J. Clement, J. Kim, and E. S. Verry, "Eddy correlation measurements of methane flux in a northern peatland ecosystem," *Boundary-Layer Meteorol.* **58**, 289–305 (1992).
- G. C. Edwards, H. H. Neumann, G. den Hartog, G. W. Thurtell, and G. Kidd, "Eddy correlation measurements of methane fluxes using a tunable diode laser at the Kinosheo Lake tower site during the northern wetlands study (NOWES)," *J. Geophys. Res.* **99**, 1511–1517 (1994).
- P. Werle and A. Popov, "Application of antimonide lasers for gas sensing in the 3–4- μ m range," *Appl. Opt.* **38**, 1494–1501 (1999).
- See, for example, P. Werle, "A review of recent advances in semiconductor laser based gas monitors," *Spectrochim. Acta Part A* **54**, 197–236 (1998), and 183 references therein.
- P. Werle, B. Scheumann, and J. Schandl, "Real-time signal-processing concepts for trace-gas analysis by diode-laser spectroscopy," *Opt. Eng.* **33**, 3093–3108 (1994).
- E. Othaki and T. Matsui, "Infrared device for simultaneous measurement of fluctuations of atmospheric carbon dioxide and water vapor," *Boundary-Layer Meteorol.* **24**, 109–114 (1982).
- C. J. Moore, "Frequency response corrections for eddy correlation systems," *Boundary-Layer Meteorol.* **37**, 17–32 (1986).
- E. K. Webb, G. I. Pearman, and R. Leuning, "Correction of flux

- measurements for chemistry effects due to heat and water vapour transfer," *Q. J. R. Meteorol. Soc.* **106**, 85–100 (1980).
32. R. T. McMillen, "An eddy correlation technique with extended applicability to nonsimple terrain," *Boundary-Layer Meteorol.* **43**, 231–239 (1988).
 33. T. Foken, R. Dlugi, and G. Kramm, "On the determination of dry deposition and emission of gaseous compounds at the biosphere–atmosphere interface," *Meteorol. Z.* **4**, 91–97 (1995).
 34. W. H. Press, S. A. Teukolsky, W. T. Vetterling, and B. P. Flannery, *Numerical Recipes in C* (Cambridge U. Press, Cambridge, 1988).
 35. F. G. Wienhold, H. Frahm, and G. W. Harris, "Measurements of N₂O fluxes from fertilized grassland using a fast response tunable diode laser spectrometer," *J. Geophys. Res.* **99**, 16557–16563 (1994).
 36. J. C. Kaimal, J. C. Wyngaard, Y. Izumi, and O. R. Coté, "Spectral characteristics of surface-layer turbulence," *Q. J. R. Meteorol. Soc.* **98**, 563–589 (1972).
 37. P. Werle, R. Kormann, R. Mücke, Th. Foken, G. Kramm, and H. Müller, "Analysis of time series data: a time domain stability criterion for stationarity tests," in *Proceedings of the EUROTRAC Symposium 1996*, P. M. Borrell, P. Borel, T. Cvi-
tas, K. Kelly, and W. Seiler, eds. (Computational Mechanics, Southampton, UK, 1996), pp. 703–707.
 38. P. Werle, R. Mücke, and F. Slemr, "The limits of signal averaging in atmospheric trace gas monitoring by tunable diode laser absorption spectroscopy," *Appl. Phys. B* **57**, 131–139 (1993).
 39. P. Schuepp, M. Y. Leclerc, J. I. McPherson, and R. L. Dejar-
dins, "Footprint prediction of scalar fluxes from analytical solutions of the diffusion equation," *Boundary-Layer Meteorol.* **50**, 355–359 (1990).
 40. M. S. Zahniser, D. D. Nelson, J. B. McManus, and P. L. Ke-
bian, "Measurement of trace gas fluxes using tunable diode laser spectroscopy," *Philos. Trans. R. Soc. London Ser. A* **351**, 371–382 (1995).
 41. O. A. Folorunso and D. E. Rolston, "Spatial variability of field-
measured denitrification gas fluxes," *Soil Sci. Soc. Am. J.* **48**, 1214–1218 (1984).
 42. M. A. K. Kahlil, R. A. Rasmussen, M. J. Shearer, R. W. Dal-
luge, L. Ren, and C. L. Duan, "Factors affecting methane emis-
sions from rice fields," *J. Geophys. Res.* **103**, 25219–25231 (1998).